Facies (2026) 72:26
https://doi.org/10.1007/s10347-026-00739-3

ORIGINAL ARTICLE

# Are Miocene-age enigmatic carbonates in the incipient Red Sea of microbial origin? A morphological study

**Hildegard Westphal**[1,2,3] · **Guillem Mateu-Vicens**[4,5] · **Elisa Garuglieri**[3] · **Anna Merkel**[6] · **Marco Taviani**[7,8] · **Jan-Peter Duda**[9]

Received: 1 April 2026 / Accepted: 18 June 2026


**Abstract**
Hitherto undescribed fine-grained carbonate deposits of inferred microbial origin unconformably rest atop a truncated basement complex along the western coastline of northwestern Saudi Arabia. These carbonates form drapes on the basement complex as well as mounds aligned along a dominant fracture direction (ENE-WSW strike). They are directly overlain by uppermost Burdigalian to Langhian strata of the Wadi Waqb Member (Jabal Kibrit Formation), which feature the earliest coral bioherms associated with the nascent Red Sea, suggesting an early to middle Miocene age for the underlying putative microbialites. Outcrop geometries reveal that the carbonate unit has undergone no significant post-depositional tilting and is largely preserved at its original depositional angle (up to 35°). Thin-section petrography and X-ray diffraction (XRD) analysis confirm that the carbonates are predominantly composed of dolomite. Micromorphological features, including textures consistent with mineralized extracellular polymeric substances (EPS), and capsule-like forms reminiscent of bacterial remains, closely resemble those found in microbialites from modern hypersaline or highly alkaline lacustrine environments. Similarly, crystal splays resemble occurrence in the fossil record that have been interpreted to be indicative of high-alkalinity conditions. Taken together, the observations suggest a restricted environment characterized by elevated levels of salinity and/or alkalinity during the early stages of Red Sea rifting and underline that microorganisms played a significant role in carbonate deposition during this stage. The stratigraphic relationship between the microbialites and the overlying coral-bearing deposits indicates that the basin evolved into a fully marine environment in the late Burdigalian.

**Keywords** Red Sea · Miocene · Microbialites · Anomalohaline basin

✉ Hildegard Westphal
hildegard.westphal@leibniz-zmt.de

[1] Leibniz Centre for Tropical Marine Research (ZMT), Fahrenheitstraße 6, 28359 Bremen, Germany

[2] Department of Geosciences, University of Bremen, Klagenfurter Straße 2-4, 28359 Bremen, Germany

[3] Physical Science and Engineering Division, King Abdullah University of Science and Technology (KAUST), Thuwal 23955-6900, Kingdom of Saudi Arabia

[4] Department of Biology and Geology, Universitat des Illes Balears, Cra. de Valldemossa, km 7.5, 07122 Palma (Illes Balears), Spain

[5] MUCBO | Museu Balear de Ciències Naturals (FJBS-MBCN), Cra. Palma-Port de Sóller, km 30.5, 07100 Sóller (Illes Balears), Spain

[6] GeoZentrum Nordbayern, Friedrich-Alexander-Universität Erlangen-Nürnberg, Schlossgarten 5, 91054 Erlangen, Germany

[7] ISMAR-CNR, Via Gobetti 101, 40129 Bologna, Italy

[8] Stazione Zoologica Anton Dohrn, Villa Comunale, 80121 Napoli, Italy

[9] Department of Geobiology, Geoscience Center, Georg-August-Universität Göttingen, Goldschmidtstr. 3, 37077 Göttingen, Germany

Published online: 21 July 2026

## Introduction

The Red Sea basin started to rift during the Early Oligocene with a second rapid rifting phase in the Late Miocene (Augustin et al. 2021; Rasul et al. 2015; Camp and Roobol 1992; Stern and Johnson 2019), leading to the formation of half-graben structures (Stephen et al. 2005; Tubbs et al. 2014). The reconstruction of the environmental development during the rifting is based on fragmentary sedimentary evidence from outcrops and boreholes (Fig. 1; e.g., Bosworth 2015). Early sedimentation in the rift graben during the Late Oligocene to Early Miocene (Chattian-Aquitanian, i.e. roughly 25-20 million years ago, myr) is characterized by thin continental red beds, overlain by Aquitanian shallow to marginal marine conglomerates, sands, and mudstones (Hughes and Johnson 2005). The first marine (partly microbial) carbonate deposits have been reported from the Aquitanian Musayr Formation in the Midyan area, that are coeval with evaporites of the Yanbu Formation deposited farther south (Fig. 1; Hughes 2014; Koeshidayatullah et al. 2016).

In the Burdigalian (roughly 20-15 myr), a major marine incursion into the northern Red Sea occurred from the Mediterranean (Bosworth et al. 2005; Segev et al. 2017; Pensa et al. 2025), initiated by the colonization by corals and the formation of extensive carbonate deposits in the incipient ocean (in Saudi Arabia: Wadi Waqb Member, Jabal Kibrit Formation, Fig. 1, e.g., Hughes 2014; Pisapia et al. 2024; Mateu-Vicens et al. 2026; in Egypt: Purser et al. 1996; Perrin et al. 1998). More specifically, coral taxa migrated into the northern Red Sea through the connection from the Mediterranean during the Burdigalian (Pisapia et al. 2024), thriving in the mesophotic zone on the flanks of the slopes of the incipient ocean basin (Mateu-Vicens et al. 2026, and references therein). New biostratigraphic data based on benthic foraminifera constrain the Wadi Waqb Member and thus the first coral colonization of the Red Sea to a latest Burdigalian age (Mateu-Vicens et al. 2026).

Notably, in the study area, the Burdigalian coral-dominated deposits are underlain by as yet undescribed sheets of fine-grained dolomitic carbonates. These carbonates unconformably overlie the truncated Precambrian basement and siliciclastic sediments assigned to an early Miocene age (Hughes 2014; Al-Kahtany 2017) and have the potential to provide important insights into the initial evolution of the early syn-rift Red Sea basin. However, despite their environmental and geodynamic significance, these dolomitic carbonates have not been investigated so far.

The coral bioherms of the Wadi Waqb Member vanished during the Late Serravallian (<12 myr; Fig. 1), likely in response to tectonic movements that isolated the Red Sea from the open ocean, leading to hypersaline conditions (Bruckner et al. 2013; Segev et al. 2017). The formation of thick evaporite deposits (Kial and Mansiyah formations), locally reaching 2500 metres in thickness (Orszag-Sperber et al. 1998), marks a salinity phase that began roughly ten million years before the Messinian Salinity Crisis in the Mediterranean (Bosworth et al. 2020; Torfstein and Steinberg 2020). Stromatolites and evaporites at the top of the carbonate succession have been described mainly from the northwestern (Egyptian) side of the Red Sea (e.g., Burchette 1988; Orszag-Sperber et al. 1998; Purser and Plaziat 1998), and they are also reported from the northernmost part of the eastern Red Sea margin (i.e., the Midyan area) (Pensa et al. 2025). Normal marine conditions were re-established in the Red Sea during the Pliocene through a connection to the Indian Ocean via the Bab al Mandab Strait (McClay et al. 1998). At that time, connection to the Mediterranean remained minimal to absent, because the Gulf of Suez was still closed due to tectonic uplift (Bosworth et al. 2020).

Here, we investigated previously undescribed dolomitic carbonates in the basal part of the Burdigalian Wadi Waqb Member in Saudi Arabia (Figs. 1, 2). By integrating field observations with findings from thin-section petrography, scanning electron microscopy (SEM) and X-ray diffraction (XRD), we elucidate the formation of these deposits, particularly the potential role of microbial processes, and discuss their environmental and geodynamic significance.

## Study area

The Wadi Waqb Member (Jabal Kibrit Formation, Fig. 1) occurs in discontinuous outcrops along the Saudi Arabian Red Sea coastline, extending from the Midyan area in the North to the Umluj (also known as Umm Lajj) area in the South (Hughes and Johnson 2005; Hughes 2014; Koeshidayatullah et al. 2016; Al-Kahtany 2017) (Fig. 2). The coral-rich carbonates in the upper part of the Wadi Waqb Member have previously been assigned to Burdigalian age (Hughes and Johnson 2005; Hussain and Al-Ramadan 2009; Hughes 2014; Al-Kahtany 2017), although new biostratigraphic data indicate that they may extend into the latest Burdigalian-Langhian interval (Mateu-Vicens et al. 2026). The carbonates of the lower part unconformably overlie the Precambrian crystalline basement and siliciclastic sediments assigned to the early Miocene Al-Wajh Formation (Al-Kahtany 2017).

The stratigraphy of the Miocene along the Saudi Arabian Red Sea coast is largely inferred from studies in the Midyan area on the North-Eastern Red Sea coastal area of Saudi Arabia (Hughes and Johnson 2005). Palaeo-ecological information on these deposits remains limited and is mostly derived from coral assemblages in the Wadi Waqb Member in that

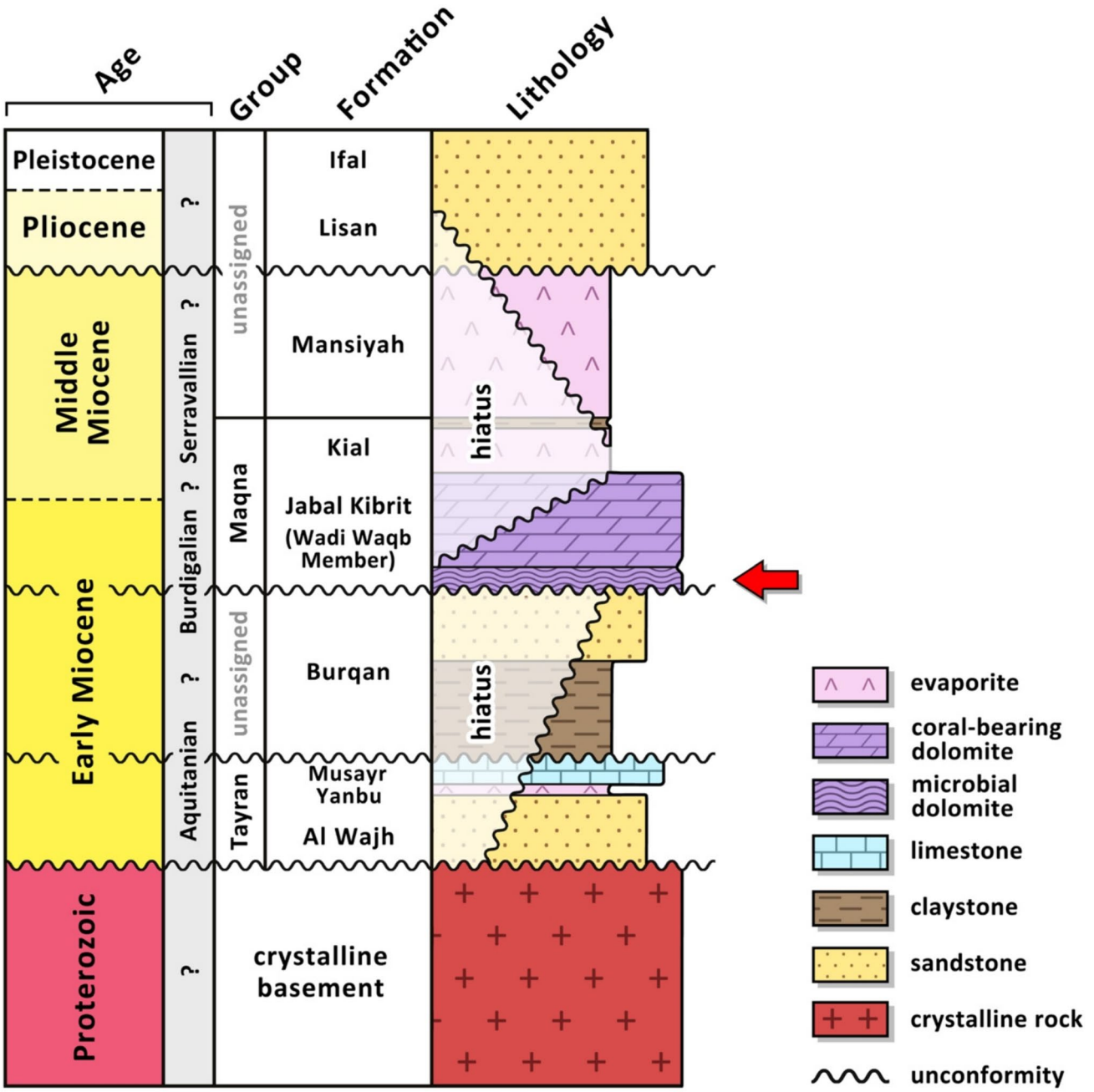


**Fig. 1** Simplified schematic stratigraphy of the north-eastern Red Sea region, after Hughes (2014). The position of the fine-grained dolomite deposits discussed here is marked by a red arrow

area, generally indicating photic, warm-water conditions (El-Sorogy et al. 2020). This was corroborated by a study of Wadi Waqb Member outcrops farther south (Pisapia et al. 2024). The present study focuses on outcrops between Umluj in the South and Al Wajh in the North (Fig. 2). These outcrops are situated in the foothills west of the flanks of the uplifted mountain range that delineates the Red Sea basin north of Umluj (25,55569° N, 37,12381° E to 25,25688° N, 37,30097° E; Fig. 2). The study area comprises discontinuous outcrops that protrude through modern desert dunes and form a distinctive double-S shape (Fig. 2b).

## Methods

Field work took place in April and October 2022, as well as in January and April 2023. After reconnaissance, description and photographic documentation of the outcrop geometries,

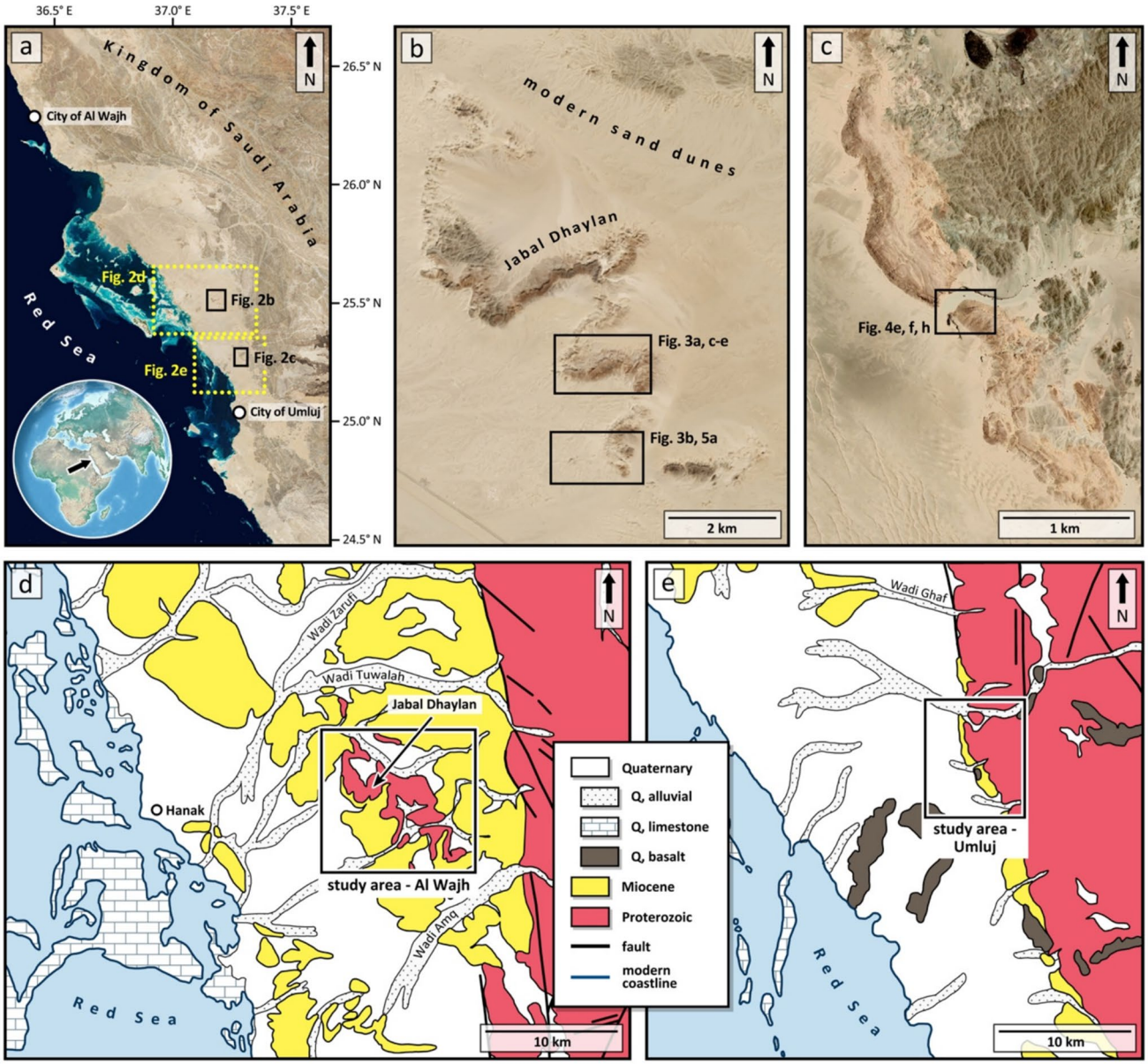


**Fig. 2** (**a**) Study area along the Saudi Arabian Red Sea coast north of the town of Umluj; arrow on globe indicates position of satellite image; (**b**) Close-up of the Al-Wajh site where the Wadi Waqb Member is surrounded by modern sand dunes, locations of Fig. 3 are indicated; (**c**) Close up of the Umluj site where the Wadi Waqb Member overlies Proterozoic basement; (**a-c**) Satellite imagery from Sentinel-2, Copernicus Sentinel data [2024]; (**d**) Simplified geological map of the Al Wajh site; (**e**) Simplified geological map of the Umluj site; (**d**, **e**) Maps based on Pellaton (1982)

systematic sampling was undertaken to investigate the facies distribution and stratigraphy.

In order to support the interpretation of the outcrops, a series of unmanned aerial system (UAS) surveys were conducted in March 2023.

A total of 36 thin sections were prepared for textural analysis of the microbialite unit (18 embedded in blue resin for highlighting porosity), polished to 40 µm thickness, and studied with a petrographic microscope in polarized light. For a more detailed analysis, eight samples were investigated by means of scanning electron microscopy (SEM). Prior to analysis, the SEM samples have been cut perpendicular to the laminae and polished with corundum powder (borcarbid 400 and 600). The sample surfaces were cleaned in an ultrasonic bath and rinsed with Millipore water. Subsequently, the surfaces were etched with 0.3% (0.1 N) hydrochloric

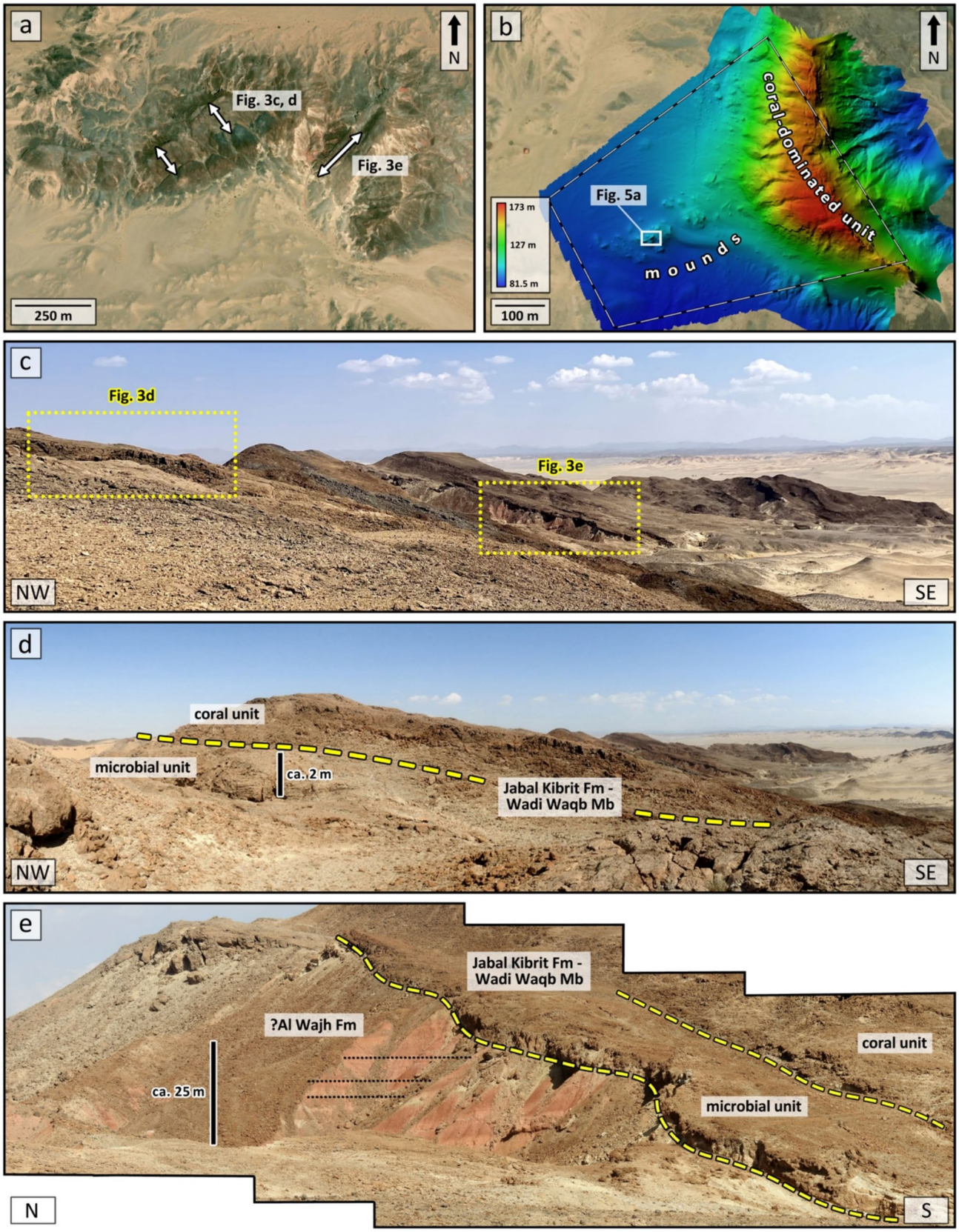
a
N
Fig. 3c, d
Fig. 3e
250 m
b
N
coral-dominated unit
Fig. 5a
173 m
127 m
81.5 m
mounds
100 m
c
Fig. 3d
Fig. 3e
NW
SE
d
coral unit
microbial unit
ca. 2 m
Jabal Kibrit Fm - Wadi Waqb Mb
NW
SE
e
Jabal Kibrit Fm - Wadi Waqb Mb
?Al Wajh Fm
coral unit
ca. 25 m
microbial unit
N
S

**Fig. 3** Outcrops of fine-grained carbonate deposits at the Al Wajh site. (**a**) Satellite image of outcrops of the fine-grained carbonate unit being overlain by the coral unit of the Wadi Waqb Member. Position of (**c**, **d**, **e**) are indicated. White arrows indicate the lateral extension of the fine-grained carbonate drape. Satellite imagery from Sentinel-2, Copernicus Sentinel data (2024) (**b**) Geomorphology image from unmanned aerial system (UAS) survey of a chain of microbialite-like mounds at the base of the coral-dominated unit of the Wadi Waqb Member, roughly aligned along the regionally dominant fault direction of the Zabargad Fracture Zone (ENE-WSW). Position of (5 **a**) is indicated; (**c**) Field aspect of the Wadi Waqb Member overlying siliciclastic basement. Positions of (**d**, **e**) are indicated. (**d**) Field aspect of the fine-grained carbonate unit overlain by the coral-dominated unit of the Wadi Waqb Member; (**e**) Field aspect showing the contact between horizontal siliciclastic rocks at the base and the fine-grained lowermost carbonate drapes of the Wadi Waqb Member atop

acid for 20 seconds, dried, and coated with iridium (10 nm). SEM analysis was performed with a Teneo-VS SEM available at KAUST Imaging and Characterization Core Lab.

For mineralogy, X-ray diffraction (XRD) analyses were conducted at the Crystallography and Geomaterials Research Group, Department of Geosciences, University of Bremen. Five dried bulk samples (Supplementary Materials Table 1) were ground to a fine powder (<20 µm particle size) and prepared with a Philips backloading system. For XRD analysis, a Bruker D8 Discover diffractometer was used. The instrument was equipped with a Cu-tube ($k_\alpha$ 1.541 Å, 40 kV, 40 mA) and a fixed divergence slit of ¼°, and monochromatization via energy discrimination on the highest resolution Linxeye detector system. Measurements were performed as continuous scans from 3 to 65° 2θ, with a calculated step size of 0.016° 2θ. Mineral identification was conducted with the Philips software X'Pert HighScore™ Vs. 1.2 (Degen et al. 2014). The determination of well-crystallized minerals like quartz, calcite or aragonite has a standard deviation of ± 1-3 % (Hardy and Tucker 1988; Vogt et al. 2002).

## Results

### Outcrop geometries

The fine-grained basal carbonate unit of the Wadi Waqb Member is well exposed in the study area (Fig. 2). Based on morphology, the fine-grained carbonate deposit can be differentiated into drapes and mounds. The drapes form layers, up to 5 m thick, atop the basement complex that consists of crystalline rocks and older Miocene siliciclastic sediments (Fig. 3). Whereas the base of the fine-grained carbonate drapes is distinct and marks an unconformity (Fig. 3c), the top of the unit is less well defined and grades into a coral-dominated carbonate unit with coral bioherms embedded in bioclastic sediment, indicating normal-marine conditions (Pisapia et al. 2024). The overall geometry of the fine-grained carbonate drapes shows a southeast-ward dip of up to 35°, contrasting with the nearly horizontal bedding of the underlying Lower Miocene siliciclastic strata (Fig. 3c). The carbonate drapes are observed to remain equally thick along the ramp slope, stretching over at least 150 m along strike and 75 m in a downslope direction in the outcrops (Fig. 3b, c). The exposure is spatially limited upslope by erosion (Fig. 3a), and downslope by a cover of younger sediment or modern sand dunes, implying that the true extension of the drapes might stretch over even larger distances.

In the lower part of the outcrops, locally non-stratabound and commonly vertically-oriented mound structures are present, forming chains of 10s of m length and 1-2 m in height that appear to follow tectonic fractures aligned to the regional Zabargad Fracture Zone (cf. Petrovic et al. 2023) (Fig. 3d, e). In the following, the facies and textures of the drapes and the mounds are described separately (see Table 1).

### Macrofacies

#### Drapes

The fine-grained drapes consist internally of decimetre-thick layers with irregular to wavy boundaries. The surfaces of individual layers show irregular, wavy to bulbous patterns. Individual bulbs reach about a decimetre in diameter (Fig. 4a-e). In cross section, these layers are formed by stacks of successive precipitates showing clear boundaries, and in some cases, darker bases (Fig. 4e). Locally, the bulbous patterns co-occur with fans of elongate crystal-like features. Generally, the drapes consist of dense lithologies with low visible porosity and a low content of clastic grains. Biogenic grains are generally rare throughout the carbonate deposits. Scarce miliolids and planktic foraminifers are limited to the upper part.

#### Mounds

The mound-shaped carbonate deposits exhibit large-scale bulbous (Fig. 5a, b) to vertical chimney-shaped structures of several decimetres in diameter, reaching up to a metre in height (Fig. 5c). Some chimney-shaped structures show internal lamination, whereas incorporated clastic grains are rare (Fig. 5c). The surfaces of the mound-shaped carbonate deposits are irregular and knobbly to pustular (Fig. 5b). Vertically broken sections macroscopically reveal a dense lithology with mm-scale clotted (i.e. thrombolitic) internal textures, commonly succeeded by several cm-thick dense crusts that show lamination or radial crystal bundle features (Fig. 5d-f).

**Table 1** Schematic of the different scales of observations from geometries, macrofacies and microfacies to ultrafacies for drapes and mounds. For further explanation see text

| | Drapes | Mounds |
|---|---|---|
| Occurrence | Cover the unconformity between Wadi Waqb Member and underlying basement complex (Fig. 3a, c-e). Equal thickness of several meters over distances of tens of meters, stacked layers of thickness of about 1 m. 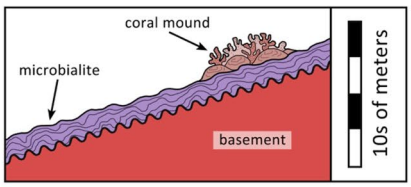  | Aligned at the toe of exposed ramp slopes, following the direction of the Zabargad Fracture Zone (Fig. 3b, 5a). 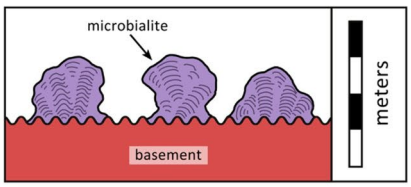  |
| Field appearance and macrofacies | Internal structure of stacked dense layers of several cm in thickness, parallel to direction of drapes. Bulbous surfaces (Fig. 4). 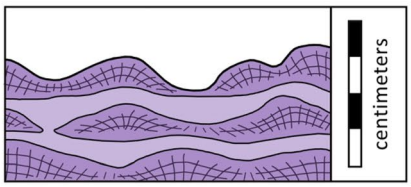  | Mound and chimney-shaped, layers growing in all directions. Typical thrombolitic inner part and dense outer part of the decimeter thick layers (Fig. 5). 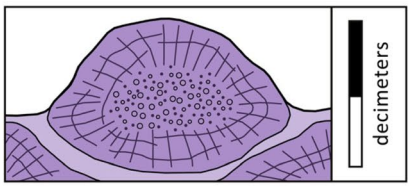  |
| Microfacies (thin sections) | Thrombolitic, extremely rare miliolids and planktic foraminifers (Fig. 6). 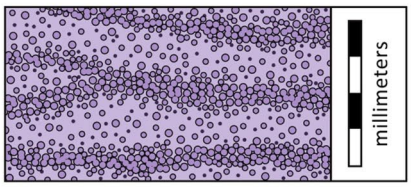  | Thrombolitic and fans of crystals, peloidal layers (Fig. 7). 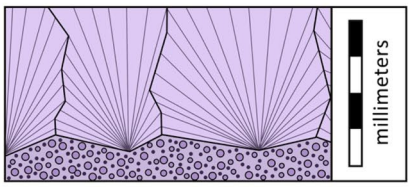  |
| Ultrafacies (SEM) | Peloidal texture and globular structures, remains of mineralized EPS-like substances (Fig. 8a-f; 9f). 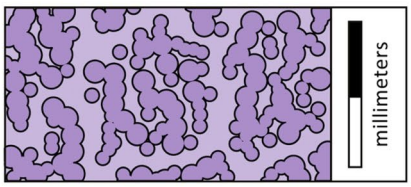  | Peloidal structures, stacked to form what appear as fans of crystals, mineralized EPS-like substances. Texture shows characteristics of biofilm with arrangement of globular structures (Fig. 8g-l; 9a-e). 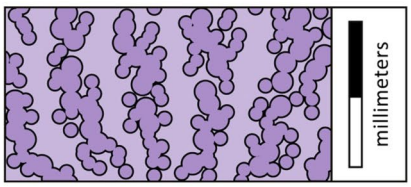  |

## Microfacies

### Drapes

Thin sections of the drapes show clotted textures and radial-crystalline splays. The clotted textures are characterized by clots approximately 50 µm in diameter. In some thin sections, mm-scale layers with clotted textures (with cement filling space between clots) alternate with dense micrite layers (Fig. 6a), locally intergrown with crystalline precipitates (Fig. 6b). These crystalline precipitates can merge into layers of dense bundles of crystals (Fig. 6c). The only biotic grains observed are local accumulations of miliolids and sporadic planktic foraminifers (Fig. 6d). Although their preservation

is poor, taxa such as *Praeorbulina glomerosa, Globigerinoides* aff. *ruber, Trilobatus trilobus* and *T. bisphericus*, have been identified, whose occurrence is consistent with a Burdigalian to Langhian age (cf. Mateu-Vicens et al. 2026).

#### Mounds

Within the mound-shaped features, clotted textures are present that can form a dense lithology lacking clear lamination (Fig. 7a). In the mounds, radial-crystalline splays are the dominant texture. They are composed of bundles of elongate crystal-like shapes up to several cm in length (Fig. 7b, c). These splays can form fans that grow to form continuous layers (Fig. 7c). Typically, the clotted textures are genetically succeeded by radial-crystalline crusts, whereas the opposite also occurs but is less common (Fig. 7d). Locally, pores are occluded by late diagenetic sparry calcite cement.

### Ultrafacies

#### Drapes

SEM analysis revealed that the textures of drapes display small-scale heterogeneity, characterized by domains with clotted, thrombolitic textures, alternating with denser patches featuring fine needles and fine-grained cement (Fig. 8a, b). At higher magnification, the clotted regions, particularly within pore spaces and their fillings, contain aggregates of globular biomorphs (Fig. 8b-d). These structures range from ~5 µm to ~50 µm in diameter. In cross-section, these structures can appear hollow (Fig. 8b, yellow arrows), with some of them showing a mineralized core partially filling the internal space (Fig. 8d). The external mineralized walls are well defined, measuring approximately 2 µm thick (Fig. 8d). In the smaller structures, an additional coating of irradiant fine needles (0.5-1 µm) is observed (Fig. 8c, d).

Notably, sheet-like structures morphologically resembling calcified extracellular polymeric substances (EPS; cf. Dohnalkova et al. 2011) are widespread in all samples, in many cases embedding fibrous elongated crystals (Fig. 8e, f). No biodetrital carbonate grains were identified, though local siliciclastic grains appear encrusted within the micritic matrix.

#### Mounds

Like the drapes, the SEM analyses of the mound structures (Fig. 8g-l) exhibit small-scale heterogeneity. They also show porous clotted, thrombolitic parts and denser ones featuring fine needles and fine-grained cement (Fig. 8g). Additionally, the clotted regions contain aggregates of globular biomorphs (Fig. h-k), most of which are larger than those observed in the drapes, reaching up to ~100 µm in diameter. Such globular structures are particularly abundant in mound and chimney-like samples, where they occur piled in multilayers to form elongate pseudo-crystals, locally dominating the rock fabric and significantly contributing to its overall texture and porosity (Figs. 8g-j, 9a-c). Again, the globules are hollow (Fig. 8i-l), or exhibit mineralized partial fillings (Fig. 8j, l). As in the drape samples, the mound samples show widespread sheet-like structures resembling calcified EPS (cf. Dohnalkova et al. 2011), embedding fibrous elongated crystals (Figs. 8k; 9d, f). The samples from the mounds are also devoid of biodetrital carbonate grains.

### Mineralogy

XRD analyses (Supplementary Materials Table 1) reveal that the carbonate composing the carbonates of drapes and mounds consist of up to 99% dolomite with varying amounts of calcite that petrographically has been determined as a late cement. In addition, traces of phyllosilicates, other silicates, apatite and gypsum have been identified.

## Discussion

### Signatures of microbial activity

This study provides the first detailed description of putative microbialites in the basal part of the Burdigalian-Langhian Wadi Waqb Member on the Red Sea coast of Saudi Arabia, directly overlying older Miocene siliciclastics and Precambrian crystalline basement. The overall geometry of the fine-grained carbonate drapes follows the pre-existing erosional morphology of the basement that dips basinward by up to 35° The underlying horizontal sedimentary layers of the basement complex (Fig. 2c) indicate that non-significant post-depositional tectonic tilting has taken place, suggesting that the uniform downslope thickness is a depositional feature.

Although substantial progress has been made in understanding the geomicrobiology of carbonate microbialites and their use as archives of past environmental conditions and microbial processes, the interpretation of fossil microbialites remains challenging, requiring robust and informative biosignatures such as morphological features indicative of microbial activity (microbial textures, relics of microorganisms) or hydrocarbon derivatives of biolipids produced by – and diagnostic of – specific organisms ("organic biomarkers") (Riding 2002; Shen et al. 2018; Suarez-Gonzalez et al. 2019; Pei et al. 2024). While initial organic biomarker analyses of the fine-grained dolomites examined here were unsuccessful (own unpublished data 2025), morphological

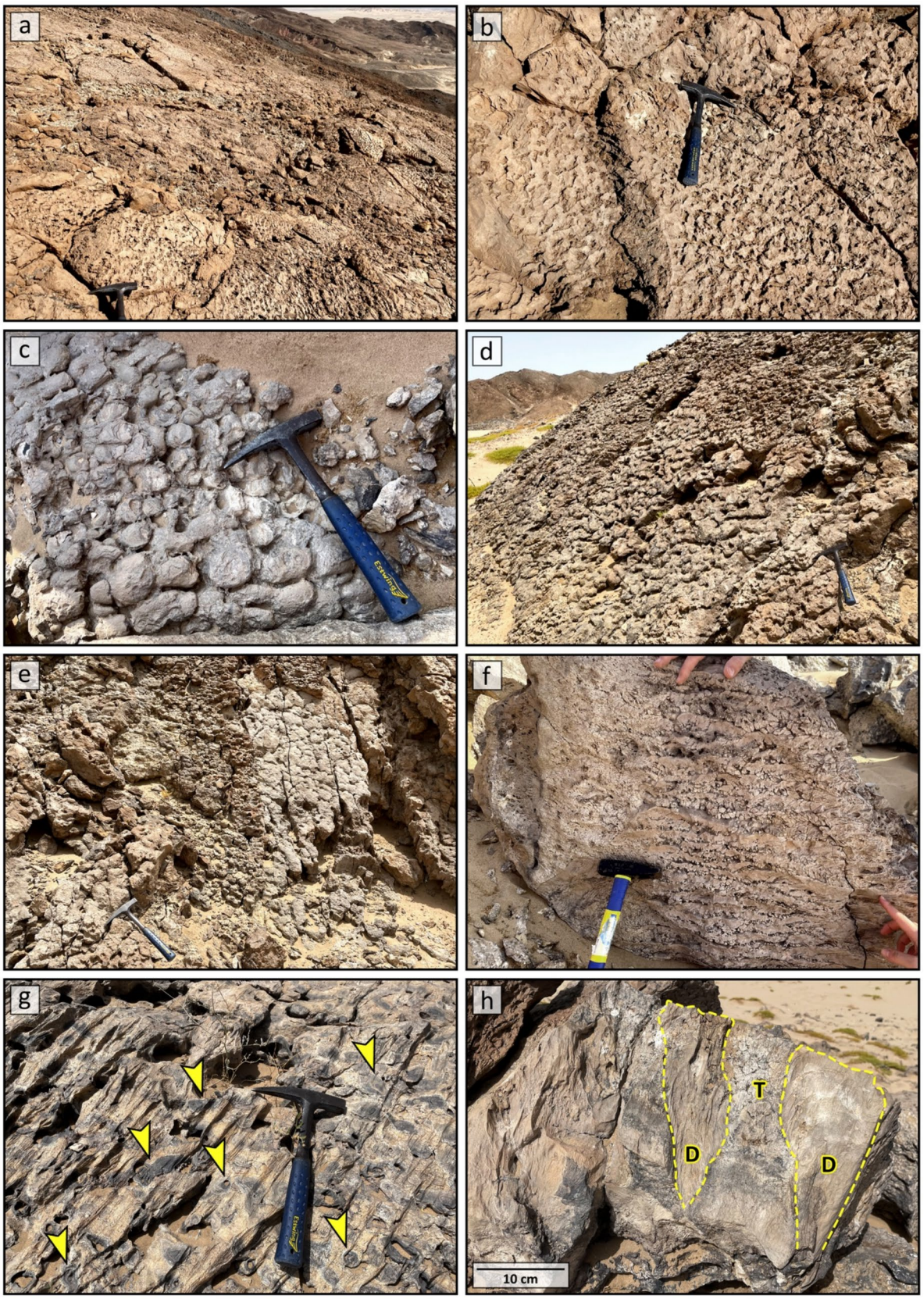
a
b
c
d
e
f
g
h
T
D
D
10 cm

**Fig. 4** Morphologies associated with the carbonate drapes at the study sites. (**a**) Drape stretching along the slope with wavy upper surface; (**b**) Close-up of the wavy surface; (**c**, **d**) bulbous surfaces; (**e**) Stacked layers of fine-grained carbonates forming a drape; (**f**, **g**) Cross sections revealing the stacked layers; (**h**) Splays embedded in bulbous structures. Hammer head is 18 cm long. (**e**, **h**) Umluj site, all others: Al Wajh site

biosignatures are preserved in great detail. For instance, the observed aggregates of globular structures in clotted regions (Fig. 8b-d, h-k) are compatible with mineralized and fossilized bacterial colonies (cf. Westall et al. 2000; Arp et al. 2003; Riding 2002). In drape samples, these structures occur predominantly as small aggregates, primarily within pore spaces, suggesting a cryptoendolithic or chasmoendolithic mode of colonization (similar to the modern cyanobacterium *Acaryochloris marina;* Behrendt et al. 2011). Observed features, including the globules and sheet-like structures, the latter resembling mineralized EPS (cf. Dohnalkova et al. 2011), are in agreement with architecturally complex calcifying biofilms (Arp et al. 1999a, b, 2003), which may have played a key role in the formation and early diagenesis of the carbonate deposits. The cross-sectional morphology of the globules is consistent with mineralized sheaths and capsules surrounding bacterial cells, particularly in association with colonial cyanobacteria (Kamennaya et al. 2012). Such protective layers, primarily composed of EPS, are, in fact, well-documented sites for carbonate precipitation in both modern and ancient settings (Arp et al.1999a, b, 2003; Kremer 2006; Kremer et al. 2012; Kazmierczak et al. 2012; Al-Bassam and Halodova 2018; Pei et al. 2024). The inner cores may represent remnants of intracellular prokaryotic structures, such as cell walls and membranes, which are also susceptible to biomineralization (Schultze-Lam et al. 1996; Boyan et al. 2020; Garuglieri et al. 2024). Based on the size, morphology, and spatial distribution of the globules observed under SEM, these structures are provisionally interpreted as monospecific coccoid bacterial colonies.

One possible interpretation is that the coccoid bacteria are cyanobacteria. A potential presence of cyanobacterial remains in the microbialites as in Fig. 8 would not be surprising as these microorganisms are known to be ecologically versatile. More specifically, cyanobacteria can thrive under euphotic to oligophotic conditions and may be partly mixotrophic (Keesing et al. 2012; Sellanes et al. 2021; Jung et al. 2023; Muñoz-Marín et al. 2024). Consequently, they inhabit a wide range of environments. However, microbialites formed by microbial communities including cyanobacteria commonly exhibit considerable morphological variability across space, reflecting local variations in environmental parameters including light quality and intensity as well as hydrodynamic conditions (e.g., Zankl 1993; Andres and Reid 2006; Reid et al. 2024; Noffke and Awramik 2026). The fact that the carbonate drapes cover the slope at a roughly constant thickness (Fig. 3c), over at least 75 m in dip direction at an angle of about 35° (Fig. 3b, c), hence spanning a water depth gradient of more than 30 m, may argue against euphotic microorganisms as major components of the microbial communities that have led to the precipitation of the microbialites studied here.

The outcrop-scale morphology of the microbialites studied here, forming uniform blankets on the unconformity and mound- and chimney-like shapes following fault directions (Figs. 3d, 10), might well be explained by communities with chemoautotrophic or heterotrophic microorganisms as key components of the microbialites. As a general pattern, the migration of hydrothermal or chemically distinct fluids along faults, can enhance microbial activity and mineral precipitation as fluid flow can deliver nutrients and redox-sensitive substrates that drive the formation of localized microbial mounds and chimneys (e.g., Polgári and Gyollai 2021; Fogret et al. 2024). In this case, the mounds and chimney-type morphologies arranged along faults (Fig. 10) might reflect a seepage-related development of microbialites, where fluids related to the opening of the Red Sea might have supplied enzymatic substrates to the microbial communities in surface environments or promoted their mineralization through mixing with chemically different surface waters.

## Environmental significance of the base Wadi Waqb Member microbialites

The microbialites at the base of the Wadi Waqb Member provide a valuable record for reconstructing environmental conditions in the nascent Red Sea during the early stages of rifting. The consistent near-complete absence of bioclastic components within these microbialites, with the notable exception of local miliolids and sparse planktic foraminifers (Fig. 6d), is particularly informative in this context. Miliolids can inhabit environments ranging from normal-marine to hypersaline conditions (Murray 2006), whereas certain planktic foraminifera such as globigerinids can tolerate salinities up to 45 PSU (Schiebel and Hemleben 2017), exceeding those observed in the present-day Red Sea (ca. 37–40 PSU; e.g. Mezger et al. 2016). Hence, the presence of extensive microbialites as well as the rare and exclusive presence of miliolids and planktic foraminifera might indicate elevated salinities at the time of deposition. At the same time, the presence of planktic foraminifera indicates some connectivity between the Red Sea basin and the open ocean, despite the basin's restricted state at that time. Miliolids and planktic foraminifers were identified only in the uppermost parts of the microbialites, just below the coral unit. Thus, their occurrence likely reflects the progressive establishment of more open-marine conditions during the

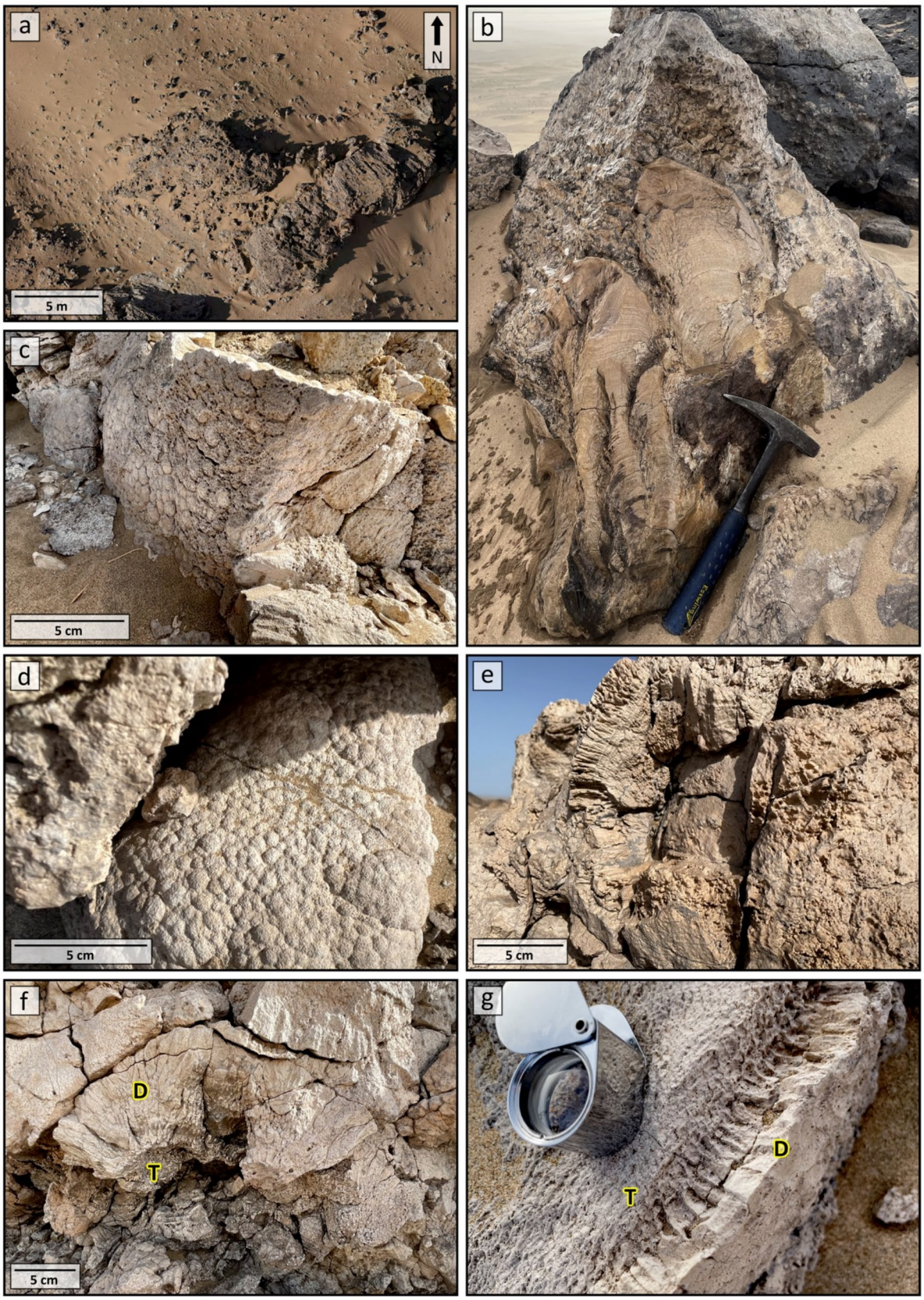
a
N
5 m
b
c
5 cm
d
5 cm
e
5 cm
f
D
T
5 cm
g
D
T

**Fig. 5** Morphologies of fine-carbonate mounds at the Al Wajh site. (**a**) Close-up image of microbial mound from UAS survey to illustrate the morphology of these biological buildups (see square in Fig. 3b for exact position). (**b**) Vertically extended mound-shaped deposit; (**c**) Bulbous shape; (**d**) Surface of a bulbous shape; (**e-g**) Cross sections revealing a clotted, thrombolitic, inner (marked by "T") and a dense outer part (marked by "D"). Hammer head 18 cm long; hand lens 2.5 cm across

Burdigalian, ultimately facilitating normal-marine environments that supported the development of coral bioherms (e.g., Perrin et al. 1998; Hughes et al. 2014; Pisapia et al. 2024). Possibly, the normal-marine water body introduced water column stratification that allowed for the planktic foraminifers to thrive coevally with the microbialites on the seafloor.

Taken together, the microbialites record an early biotic phase in the nascent Red Sea, predating its further opening in the upper Burdigalian, when the establishment of a connection to open-marine environments, particularly the Mediterranean, enabled the colonization of the Red Sea by corals and associated fauna. Microbialites have previously been reported from the top of the coral-rich Wadi Waqb Member, where in the early Langhian the connection to the Mediterranean closed tectonically, leaving the Red Sea to undergo a prolonged evaporite event that lasted until the Pliocene (e.g. Orszag-Sperber et al. 1998; Pensa et al. 2025). In the Wadi Waqb Member outcrops in the study area, the erosive top of the formation is cutting down into the coral-dominated deposits, and the contact to the sedimentary succession succeeding the Wadi Waqb Member is not preserved (Pisapia et al. 2024).

On the Egyptian side of the northern Red Sea, laminated microbialites encrusting Precambrian basement are interpreted as evidence of the early Miocene, pre-evaporite restricted marine phase in this region (Perrin et al. 1998). Similarly, a stromatolitic unit occurs atop Precambrian strata in Egypt on steep slopes along the Red Sea coast (Purser and Plaziat 1998). The morphological characteristics of the stromatolites described by these authors closely resemble those observed at the base of the Wadi Waqb Member in the outcrops studied here. Similar features include their downslope extension over distances of 20-50 m before being truncated at the top by erosion, as well as domal shapes and bulbous surfaces. However, these stromatolites occur atop the coral unit and immediately precede the evaporites precipitated during the Langhian hypersaline phase, leading to the Red Sea salinity crisis, indicating that they are in a younger stratigraphic position compared to the microbialites described here. To our knowledge, these younger occurrences have not yet been investigated from a geobiological perspective.

Crusts exhibiting strong morphological similarities to those studied here have been observed on subvertical slopes in the modern Red Sea (off Sudan: Brachert and Dullo 1991; off Saudi Arabia: Lüdmann et al. 2024). These crusts, suspected to be at least partly microbial in origin, occur in mesophotic to aphotic zones along the steep slopes of pinnacles and platforms. They display bulbous surfaces with cup-shaped, curved outer rims and sediment fill. The crusts are approximately 10,000 years old (Brachert and Dullo 1991), dating back to the deglacial period, when the previously restricted connection between the Red Sea and the Indian Ocean via the Bab-al-Mandeb strait was reopening, and hypersaline conditions were beginning to subside. Microbialites thus appear to be a recurrent feature of the Red Sea basin that is characterized by aridity and restricted connection to the open ocean.

## Microbialites formation and authigenesis

Carbonate microbialites with stromatolitic or clotted, thrombolitic textures are known from a wide range of modern and ancient environments, and formed in subaqueous settings through a variety of processes (authigenic mineralization and/or trapping and binding) involving diverse microbial communities (Reid et al. 1999; Riding 2002; Dupraz and Visscher 2005; Warthmann et al. 2011; Suarez-Gonzalez et al. 2019; Landing and Johnson 2024). Compared to earlier periods in Earth's history (particularly the Precambrian), however, marine carbonate microbialites are relatively rare today and are mostly restricted to settings with high sediment load (e.g., the stromatolites in the subtidal zones of the Exuma Cays, Bahamas: Reid et al. 1995; Andres et al. 2006), or environments characterized by high salinity or alkalinity (Riding 2000; Peters et al. 2017).

The hydrochemical settings favoured by microbialite formation range from freshwater to hypersaline systems, with alkalinity in many cases playing a pivotal role in mineralization (e.g., Arp et al. 1999a, b, 2003; Dupraz et al. 2009; Chagas et al. 2016). Metabolism-induced carbonate precipitation is usually significant in these systems, although the underlying mineral (trans)formation processes are more complex (see e.g. Reitner et al. 1995; Trichet and Défarge 1995; Arp et al. 1999a, b, 2003; Reitner 2004; Dupraz et al. 2009; Pei et al. 2024). Regardless, classic examples of modern microbial carbonates such as the stromatolites of Shark Bay (Australia) form under elevated salinity and alkalinity (Suosaari et al. 2016). Similarly, recently documented stromatolites on the Al Wajh carbonate platform in the northern Red Sea develop in intertidal, high-alkalinity settings influenced by repeated wetting-drying cycles and exposure to extreme temperatures (Vahrenkamp et al. 2024). In this case, the role of microbial processes in carbonate formation has been confirmed through SEM imaging and DNA analysis.

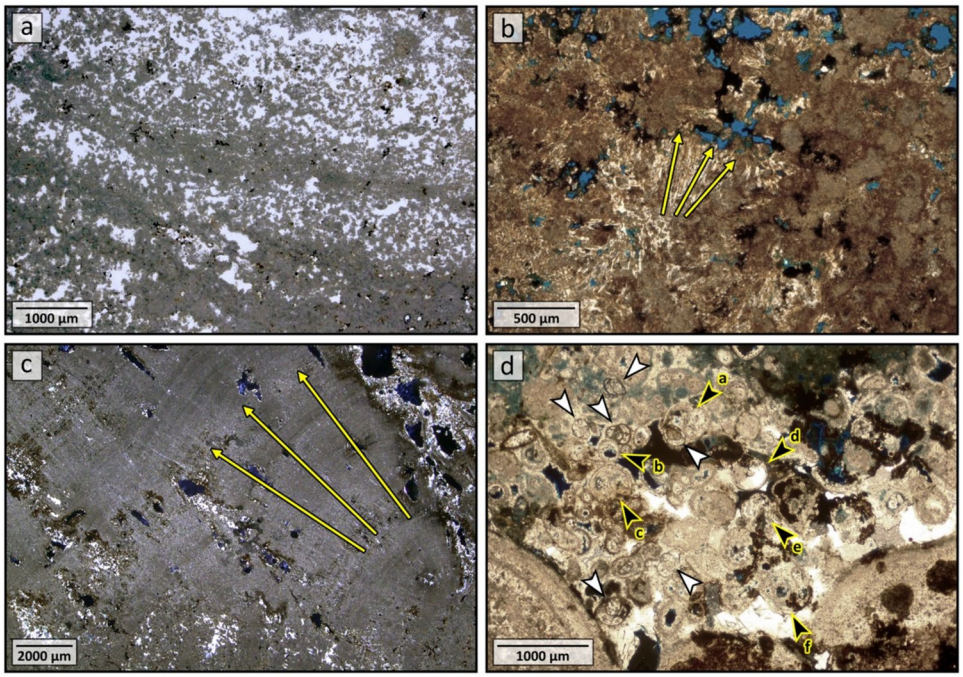


**Fig. 6** Thin-section micrographs from microbialite drapes collected at the study site. (**a**) Clotted texture; (**b**) Clotted texture, in parts associated with needle-shaped crystals (indicated by yellow arrows); (**c**) Dense micritic part with crystal splays (indicated by yellow arrows), crossed polars; (**d**) Pocket with miliolid benthic foraminifers and planktic foraminifers (white and black arrows, respectively) including [a] *Globigerinoides* aff. *ruber*, [b] *Praeorbulina glomerosa,* [c] *Trilobatus trilobus*, [d] *T. bisphericus,* [e] *G. ruber*, [f] unidentified planktic foraminifer. Blue epoxy used in (**b**) and (**d**)

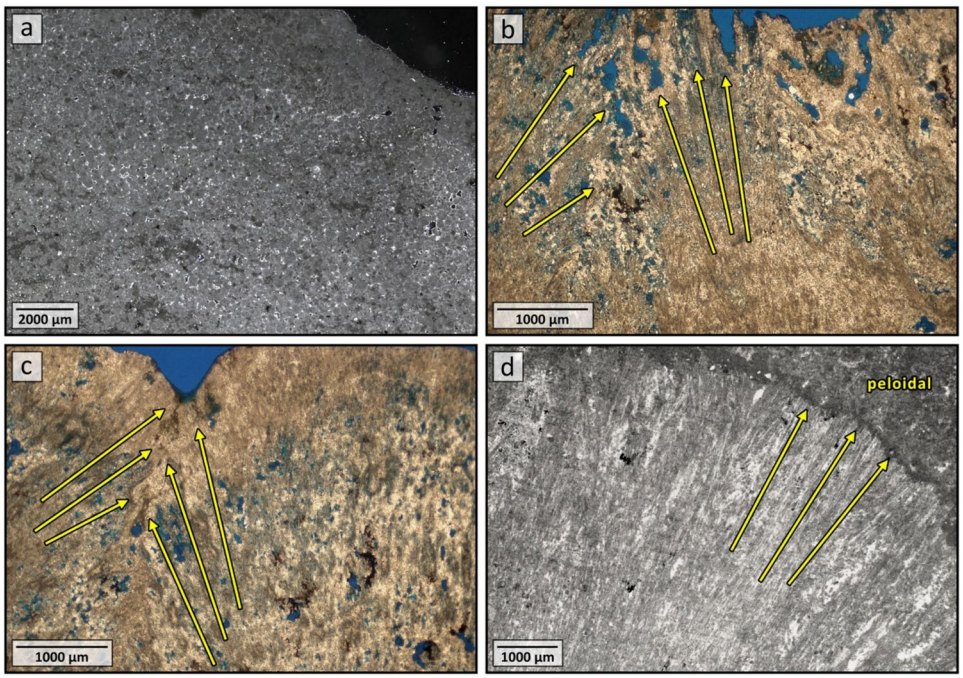


**Fig. 7** Thin-section micrographs from the carbonate mounds. (**a**) Clotted texture, crossed polars; (**b**, **c**) Crystal bundles (yellow arrows) and crystals arranged in converging fans; (**d**) Crystal bundles (yellow arrows) followed by clotted texture. Blue epoxyused in (**b**) and (**c**)

Morphologically, at both field- and macroscopic scales, the Miocene microbialites studied here appear to exhibit remarkable similarities to (microbial) carbonate deposits from other high-salinity environments (e.g. the Messinian of the Mediterranean: Arenas and Pomar 2010; Villafañe et al. 2018; Suarez-Gonzalez et al. 2019, 2022) as well as from the alkaline Pyramid Lake in Nevada (USA), which also contain fine-grained dolomite (Benson et al. 1994, 1995; Arp et al. 1999b; Benson 2004). Although these deposits require more detailed, multi-scale comparison with the Miocene microbialites investigated herein before drawing firm conclusions, this might suggest that the latter may also have formed in a hypersaline and/or alkaline environment that existed during the earliest stages of the incipient Red Sea.

A hypersaline setting would be consistent with the occurrence of primary or very early-diagenetic dolomite (cf. Vasconcelos and McKenzie 1997; Bontognali et al. 2010), which is indicated by the mimetic dolomitization

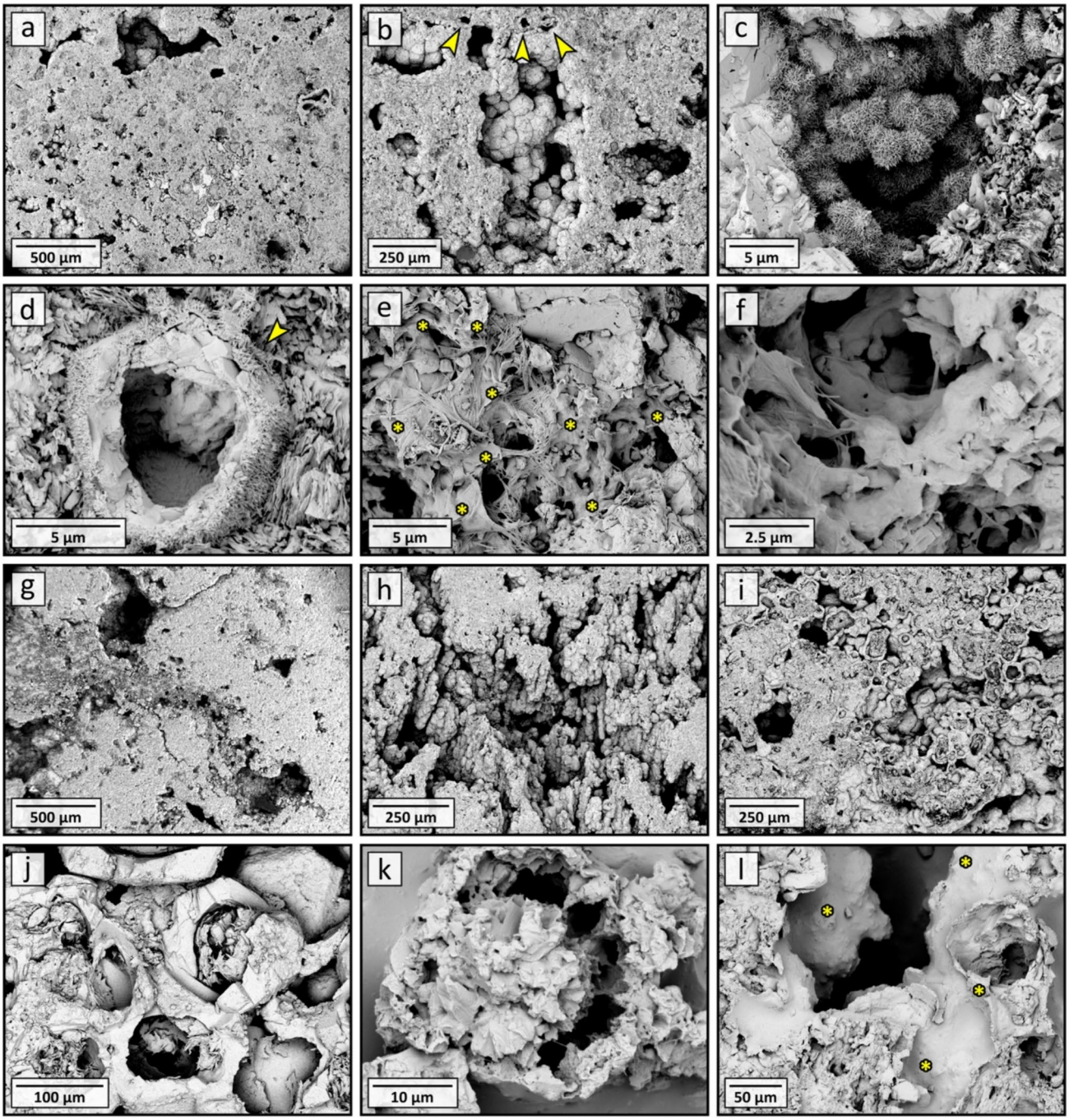


**Fig. 8** SEM micrographs of microbialites from drapes (**a**-**f**) and mound structures (**g**-**l**). (**a**) Low magnification view; (**b**) Globular structures with cross-sectioned globules indicated by yellow arrows; (**c**) Small globular structures coated by needle-shaped precipitates; (**d**) Hollow globular structure coated by needle-shaped precipitates (yellow arrow); (**e**) Sheets resembling mineralized extracellular polymeric substances (EPS) (yellow asterisks); (**f**) Details of fine-scale EPS-like sheets; (**g**) Low magnification view of sample from mound structure; (**h**) Globular structures piled in multi-layered groups; (**i**-**k**) Sectioned globular structures. (**l**) EPS-like sheets (yellow asterisks indicate the regions covered by the sheets)

of overlying corals, preserving delicate details and lacking destructive dolomite crystal growth (Pisapia et al. 2024). Stable oxygen and carbon isotopes also point to a diagenetic rather than a primary origin of the dolomite (Herlambang et al. 2022). Other examples of interest for future comparison include the high-salinity Messinian microbialites of the Mediterranean (e.g., Suarez-Gonzalez et al. 2022). Furthermore, the splays observed in the drapes and mounds macroscopically resemble fan-like crystal bundles in deposits from various ancient high-alkalinity settings, including the

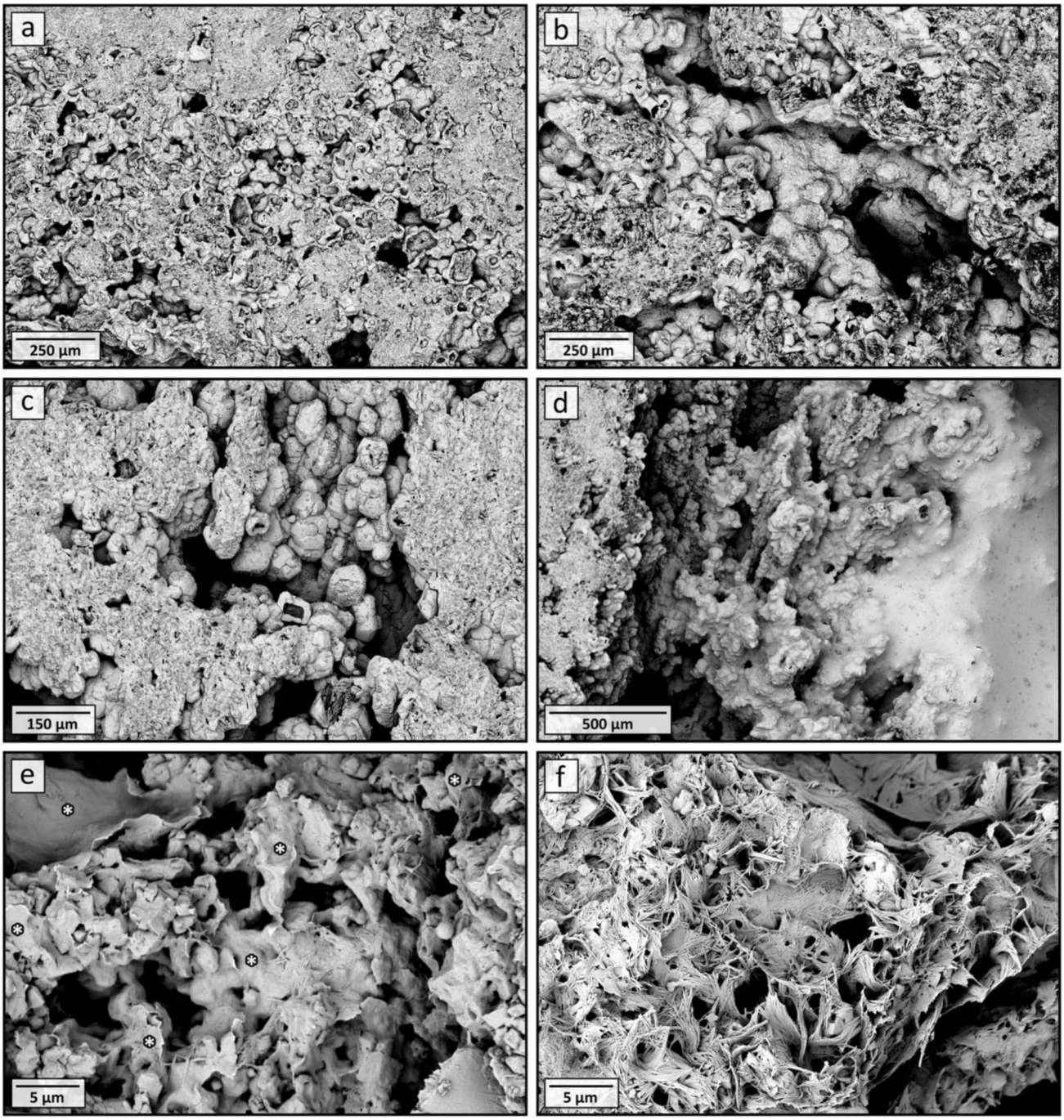


**Fig. 9** Scanning electron microscope (SEM) micrographs of biofilm-like structures. (**a**-**c**) Overview of the biofilm-like matrix dominating "chimney"-type samples; (**d**) Mineralized EPS-like sheet covering the globule piles in a "chimney"-type sample; (**e**) EPS-like sheets observed in a drape sample; black asterisks indicate the EPS-like substance; (**f**) "Chimney"-type sample containing crystal bundles

Precambrian of North America (Corsetti et al. 2004), the Triassic of Armenia (Friesenbichler et al. 2018), and the Pleistocene of Ethiopia (Jaramillo-Vogel et al. 2023). In the Ethiopian Danakil Depression, for instance, such splays have been interpreted as fibrous aragonite precipitated under extremely high alkalinity, not necessarily induced by, but co-occurring with, microbial activity, and subsequently partly or entirely replaced by calcite during diagenesis (Jaramillo-Vogel et al. 2023). While the Lower Miocene setting in the nascent Red Sea basin probably indeed exhibited high alkalinity and high salinity due to its cul-de-sac position, SEM imagery (Fig. 8h) reveals that the elongate crystals are composed of coccoid shapes interpreted as microbial relics. This is reminiscent of the elongate aggregates described by

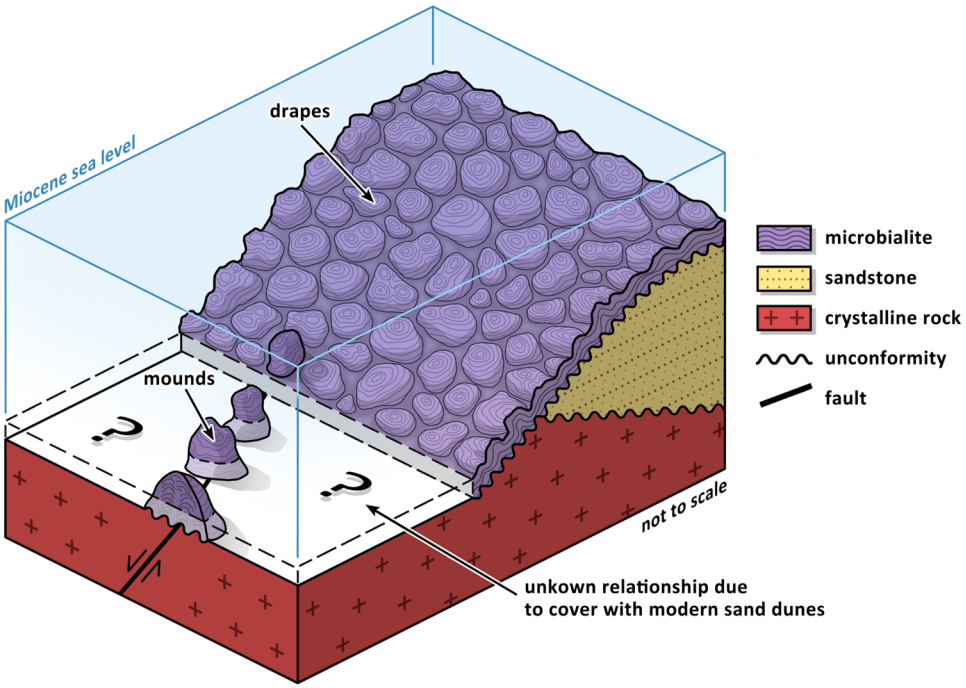


**Fig. 10** Schematic model of the depositional situation during microbialite formation. On top of the unconformity towards the basement complex, the microbialite drape covers the seafloor along the depth gradient. At the toe of slope, microbialite mounds line up along the dominant fault direction. The ecosystem is dominated by microbial carbonate precipitation, consistent with formation in a hyperalkaline and/or hypersaline environment

Friesenbichler et al. (2018) as "mimicking crystal shape" and interpreted to be of biotic origin.

Taken together, the Miocene microbialites discussed here solely formed through authigenic mineralization, as indicated by their massive crystalline fabric with few bacterial relics and a lack of detrital components. However, it remains unclear whether carbonate formation was mainly driven by metabolism or occurred rather passively by the mineralization of EPS ("organomineralization", e.g., Reitner et al. 1995; Trichet and Défarge 1995; Reitner 2004; Pei et al. 2024). Another remaining question concerns the timing of dolomitization, or whether the dolomite formed as a primary precipitate. Microbial dolomite formation remains one of the great and longstanding mysteries in carbonate sedimentology (e.g., McKenzie 1991; Krause et al. 2012; Di Loreto et al. 2019), and the microbialites analysed here may help to gain a better understanding of microbially-induced precipitation under anomalohaline conditions.

## Conclusions

This study marks the first morphological description of hitherto enigmatic, fine-grained carbonate deposits at the base of the coral-dominated upper Wadi Waqb Member along the Red Sea coast of Saudi Arabia, unconformably overlying Precambrian basement and early Miocene siliciclastics in the northern part. The carbonate deposits draping the unconformity are inferred to be microbialites of Burdigalian age. The microbial origin is evidenced by a variety of features, including sedimentological and micromorphological characteristics such as clotted textures, consistent with mineralized extracellular polymeric substances (EPS), and capsule-like features reminiscent of bacterial relics. Based on the geological setting and field geometries, as well as on the morphology and oligotypic faunal content of the microbialites, we hypothesize that the best genetic scenario for the formation of the basal microbialites of the Wadi Waqb Member involves a high-salinity and/or high alkalinity, relatively deep 'lacustrine' environment existing during the Burdigalian or earlier. The duration of this saline lake phase preceding the first coral ecosystems in the incipient Red Sea during the Burdigalian remains uncertain.

**Supplementary Information** The online version contains supplementary material available at https://doi.org/10.1007/s10347-026-00739-3.

**Acknowledgements** This contribution is dedicated to Judy McKenzie's memory whose research added an entirely new angle to microbialite research. We thank Pablo Suarez-Gonzalez and an anonymous reviewer for their constructive comments, and Maurice Tucker, Editor-in-Chief of Facies, for handling the manuscript. The authors are grateful to Red Sea Global for access to the study area, and to Alexander Petrovic, Thomas Teillet, Tihana Pensa, Chiara Pisapia, and Nicolas Boehm (all KAUST), Marlena Joppien and Lea Tabea Fuchs (University of Bremen/KAUST), Eike C. Bornholdt (University of Potsdam) and Filiz Duda (Göttingen) as well as Giorgio Castellan (ISMAR-CNR) for their help in the field. We thank Aboud al Afifi and Volker Vahrenkamp (KAUST) for providing us with useful information for preparing the field work. The unmanned aerial system (UAS) survey was undertaken by FalconViz (Thuwal, Saudi Arabia); thanks are due to Khaled Abdelgawad and his team for this collaboration. Thanks are due to Sebastian Flotow (ZMT) and Axel Hackmann, Jorinel Domingos, Teresa Williams and Malte Krömer (Göttingen University) for support with the preparation of samples. Patrick Boyden (University of Bremen) is acknowledged for providing Fig. 2. This study is part

of a larger project on the Miocene deposits of the northern Saudi Arabian Red Sea coast, funded through King Abdullah University of Science and Technology (KAUST) baseline funding to HW. GMV has been funded by the Ministerio de Ciencia e Innovación of the Spanish Government (project PID2022-137860NB-I00). This is CNR-ISMAR, Bologna, Scientific Contribution No. 2104.

**Author contributions** Project concept and funding acquisition: HW; fieldwork: HW, GMV, JPD; petrography and mineralogy: HW, EG; concept of manuscript: all authors; writing of manuscript: all authors; concept and implementation of figures: HW, AM, GMV, EG; revision of manuscript: all authors.

**Funding** Open Access funding enabled and organized by Projekt DEAL. King Abdullah University of Science and Technology baseline funding to Hildegard Westphal, Ministerio de Ciencia e Innovación PID2022-137860NB-I00 to Guillem Mateu-Vicens.

**Data Availability** Further data that support the findings of this study are available from corresponding author upon reasonable request.

## Declarations

**Conflict of interest** The authors have identified no potential sources of conflict of interest.



## References

Al-Bassam K, Halodova P (2018) Fossil bacteria in Cenomanian-Turonian phosphate nodules and coprolites, Bohemian Cretaceous Basin Czech Republic. Ann Soc Geol Pol 88:565

Al-Kahtany KM (2017) Facies development of the Middle Miocene reefal limestone in northwest Saudi Arabia. J Afr Earth Sci 130:134–140. https://doi.org/10.1016/j.jafrearsci.2017.03.012

Andres MS, Reid RP (2006) Growth morphologies of modern marine stromatolites: a case study from Highborne Cay, Bahamas. Sediment Geol 185:319–328. https://doi.org/10.1016/j.sedgeo.2005.12.020

Andres MS, Sumner DY, Reid RP, Swart PK (2006) Isotopic fingerprints of microbial respiration in aragonite from Bahamian stromatolites. Geology 34(11):973–976. https://doi.org/10.1130/G22859A

Arenas C, Pomar L (2010) Microbial deposits in upper Miocene carbonates, Mallorca, Spain. Palaeogeogr Palaeoclimatol Palaeoecol 297:465–485. https://doi.org/10.1016/j.palaeo.2010.08.030

Arp G, Reimer A, Reitner J (1999a) Calcification in cyanobacterial biofilms of alkaline salt lakes. Eur J Phycol 34(4):393–403

Arp G, Thiel V, Reimer A, Michaelis W, Reitner J (1999b) Biofilm exopolymers control microbialite formation at thermal springs discharging into the alkaline Pyramid Lake, Nevada, USA. Sediment Geol 126(1–4):159–176

Arp G, Reimer A, Reitner J (2003) Microbialite formation in seawater of increased alkalinity, Satonda Crater Lake, Indonesia. J Sediment Res 73(1):105–127. https://doi.org/10.1306/071002730105

Augustin N, van der Zwan FM, Devey CW, Brandsdóttir B (2021) 13 million years of seafloor spreading throughout the Red Sea Basin. Nat Commun 12(1):2427. https://doi.org/10.1038/s41467-021-22785-3

Behrendt L, Larkum AW, Norman A, Qvortrup K, Chen M, Ralph P, Kühl M (2011) Endolithic chlorophyll d-containing phototrophs. ISME J 5(6):1072–1076

Benson L (1994) Carbonate deposition, Pyramid Lake subbasin, Nevada: 1. Sequence of formation and elevational distribution of carbonate deposits (tufas). Palaeogeogr Palaeoclimatol Palaeoecol 109(1):55–87

Benson LV (2004) The Tufas of Pyramid Lake, Nevada: U.S. Geological Survey Circular 1267, pp 14. https://pubs.usgs.gov/circ/2004/1267/

Benson L, Kashgarian M, Rubin M (1995) Carbonate deposition, Pyramid Lake subbasin, Nevada: 2. Lake levels and polar jet stream positions reconstructed from radiocarbon ages and elevations of carbonates (tufas) deposited in the Lahontan basin. Palaeogeogr Palaeoclimatol Palaeoecol 117(1–2):1–30

Bontognali TR, Vasconcelos C, Warthmann RJ, Bernasconi SM, Dupraz C, Strohmenger CJ, McKenzie JA (2010) Dolomite formation within microbial mats in the coastal sabkha of Abu Dhabi (United Arab Emirates). Sedimentology 57:824–844

Bosworth W (2015) Geological evolution of the Red Sea: Historical Background, Review and Synthesis. In: The Red Sea. Springer. https://doi.org/10.1007/978-3-662-45201-1_3.

Bosworth W, Huchon P, McClay K (2005) The Red Sea and Gulf of Aden basins. J Afr Earth Sci 43:334–378

Bosworth W, Khalil SM, Ligi M, Stockli DF, McClay KR (2020) Geology of Egypt: The Northern Red Sea. In: Hamimi Z, El-Barkooky A, Martínez Frías J, Fritz H, Abd El-Rahman Y (eds) Geology of Egypt. pp 343–374

Boyan BD, Swain LD, Everett MM, Schwartz Z (2020) Mechanisms of microbial mineralization. In: Boyan BD (ed) Calcification in biological systems. CRC Press, Boca Raton, pp 129–156

Brachert TC, Dullo WC (1991) Laminar micrite crusts and associated foreslope processes, Red Sea. J Sediment Petrol 61:354–363

Bruckner A, Rowlands G, Riegl B, Purkis S, Williams A, Renaud P (2013) Atlas of Saudi Arabian Red Sea marine habitats. Panoramic Press, Phoenix, AZ, p 273

Burchette TP (1988) Tectonic control on carbonate platform facies distribution and sequence development: Miocene, Gulf of Suez. Sediment Geol 59:179–204

Camp VE, Roobol MJ (1992) Upwelling asthenosphere beneath western Arabia and its regional implications. J Geophys Res 97(B11):15255–15271

Chagas AAP, Webb GE, Burne RV, Southam G (2016) Modern lacustrine microbialites: towards a synthesis of aqueous and carbonate geochemistry and mineralogy. Earth Sci Rev 162:338–363. https://doi.org/10.1016/j.earscirev.2016.09.012

Corsetti FA, Lorentz NJ, Pruss SB (2004) Formerly-Aragonite Seafloor Fans from Neoproterozoic Strata, Death Valley and Southeastern Idaho, United States: Implications for "Cap Carbonate" Formation and Snowball Earth. In: The Extreme Proterozoic: Geology, Geochemistry, and Climate. Jenkins GS, McMenamin MAS, McKay CP Sohl L (eds) https://doi.org/10.1029/146GM04

Di Loreto ZA, Bontognali TRR, Al Disi ZA, Al Saad Al-Kuwari H, Williford KH, Strohmenger CJ, Sadooni F, Palermo C, Rivers JM, McKenzie JA, Tuite A, Dittrich M (2019) Microbial community

composition and dolomite formation in the hypersaline microbial mats of the Khor Al-Adaid sabkhas. Qatar Extremophiles 23(2):201–217. https://doi.org/10.1007/s00792-018-01074-4

Dohnalkova AC, Marshall MJ, Arey BW, Williams KH, Buck EC, Fredrickson JK (2011) Imaging hydrated microbial extracellular polymers: comparative analysis by electron microscopy. Appl Environ Microbiol 77(4):1254–1262

Dupraz C, Visscher PT (2005) Microbial lithification in marine stromatolites and hypersaline mats. Trends Microbiol 13(9):429–438. https://doi.org/10.1016/j.tim.2005.07.008. (**PMID: 16087339**)

Dupraz C, Reid RP, Braissant O, Decho A, Norman R, Visscher P (2009) Processes of carbonate precipitation in modern microbial mats. Earth Sci Rev 96:141–162. https://doi.org/10.1016/j.earscirev.2008.10.005

El-Sorogy AS, Tsaparas N, Al-Kahtany K (2020) Middle Miocene corals from Midyan area, Northwestern Saudi Arabia. Geol J 55(7):5594–5605. https://doi.org/10.1002/gj.3761

Fogret L, Sansjofre P, Lalonde SV (2024) Geochemistry of carbonate microbialites through time and space: insights from the microbialite collection of the Muséum National d'Histoire Naturelle (MNHN), France. Chem Geol 662:122239. https://doi.org/10.1016/j.chemgeo.2024.122239

Friesenbichler E, Richoz S, Baud A, Krystyn L, Sahakyan L, Vardanyan S, Peckmann J, Reitner J, Heindel K (2018) Sponge-microbial build-ups from the lowermost Triassic Chanakhchi section in southern Armenia: microfacies and stable carbon isotopes. Palaeogeogr Palaeoclimatol Palaeoecol 490:653–672. https://doi.org/10.1016/j.palaeo.2017.11.056

Garuglieri E, Marasco R, Odobel C, Chandra V, Teillet T, Areias C, Sánchez-Román M, Vahrenkamp V, Daffonchio D (2024) Searching for microbial contribution to micritization of shallow marine sediments. Environ Microbiol 26(2):e16573

Hardy RG, Tucker ME (1988) X-ray powder diffraction of sediments. In: Tucker ME (ed) Techniques in sedimentology. Blackwell, Oxford, p pp.191-228

Herlambang A, Koeshidayatullah AI, Amao AO, Bello AM, Al-Ghamdi F, Malik MH, Al-Ramadan KAH (2022) Structural diagenesis and dolomitization of Cenozoic post-rift carbonates in the Red Sea rift basin: a multiproxy approach. Front Earth Sci 10:1037126. https://doi.org/10.3389/feart.2022.1037126

Hughes GW (2014) Micropalaeontology and palaeoenvironments of the Miocene Wadi Waqb carbonate of the northern Saudi Arabian Red Sea. GeoArabia 19(4):59–108. https://doi.org/10.2113/geoarabia190459

Hughes GW, Johnson RS (2005) Lithostratigraphy of the Red Sea. GeoArabia 10(3):49–126

Hussain M, Al-Ramadan K (2009) Microfacies analysis of Wadi Waqb member (Miocene) in Wadi Aynunah, northwest of Saudi Arabia. Carbonates Evaporites 24:139–149

Jaramillo-Vogel D, Braga JC, Negga HA, Vennemann T, De Boever E, Schaegis JC, Rime V, Atnafu B, Kidane T, Foubert A (2023) Pleistocene aragonite crust diagenesis mimics microbialite fabrics (Danakil Depression, Ethiopia). Sediment Geol 446(24):106341. https://doi.org/10.1016/j.sedgeo.2023.106341

Jung P, Harion F, Wu S, Nürnberg DJ, Bellamoli F, Guillen A, Leira M, Lakatos M (2023) Dark blue-green: cave-inhabiting cyanobacteria as a model for astrobiology. Front Astron Space Sci 10:1107371

Kamennaya NA, Ajo-Franklin CM, Northen T, Jansson C (2012) Cyanobacteria as biocatalysts for carbonate mineralization. Minerals (Basel) 2(4):338–364

Kazmierczak J, Kremer B, Racki G (2012) Late Devonian marine anoxia challenged by benthic cyanobacterial mats. Geobiology 10(5):371–383

Keesing JK, Usher KM, Fromont J (2012) First record of photosynthetic cyanobacterial symbionts from mesophotic temperate sponges. Mar Freshw Res 63(5):403–408. https://doi.org/10.1071/MF11216

Koeshidayatullah A, Al-Ramadan K, Collier R, Hughes GW (2016) Variations in architecture and cyclicity in fault-bounded carbonate platforms: early Miocene Red Sea Rift, NW Saudi Arabia. Mar Pet Geol 70:77–92

Krause S, Liebetrau V, Gorb S, Sánchez-Román M, McKenzie JA, Treude T (2012) Microbial nucleation of Mg-rich dolomite in exopolymeric substances under anoxic modern seawater salinity: new insight into an old enigma. Geology 40(7):587–590. https://doi.org/10.1130/G32923.1

Kremer B (2006) Mat-forming coccoid cyanobacteria from early Silurian marine deposits of Sudetes. Poland Acta Palaeontologica Polonica 51(1):143–154

Kremer B, Kazmierczak J, Łukomska-Kowalczyk M, Kempe S (2012) Calcification and silicification: fossilization potential of cyanobacteria from stromatolites of Niuafo'ou's Caldera Lakes (Tonga) and implications for the early fossil record. Astrobiology 12(6):535–548

Landing E, Johnson ME (2024) Stromatolites and their "kin" as living microbialites in contemporary settings linked to a long fossil record. J Mar Sci Eng 12:2127. https://doi.org/10.3390/jmse12122127

Lüdmann T, Westphal H, Ariza-Fuentes M, Castellan G, Giovenzana F, Kappelmann Y, Marchese F, Stuhr M, Taviani M, Vahrenkamp V, Vicario S, Vittori V, Science Party (2024) Red Sea Paleoenvironmental evolution under Monsoon fluctuations in the Pleistocene to Holocene - cruise no 193. In: METEOR-Berichte. https://doi.org/10.48433/cr_m193

Mateu Vicens G, Brandano M, Boyden P, Benedetti A, Duda J-P, Westphal H (2026) Mesophotic normality: lower Miocene coral bioherms pioneering the incipient Red Sea. Palaeogeogr Palaeoclimatol Palaeoecol 696:113874. https://doi.org/10.1016/j.palaeo.2026.113874

McClay KR, Nichols GJ, Khalil SM, Darwish M, Bosworth W (1998) Extensional tectonics and sedimentation, eastern Gulf of Suez, Egypt. In: Purser BH, Bosence DWJ (eds) Sedimentation and tectonics in rift basins: Red Sea–Gulf of Aden. Chapman & Hall, London, pp 223–238

McKenzie JA (1991) The dolomite problem: an outstanding controversy. In: Muller DW, McKenzie JA, Weissert H (eds) Controversies in modern geology. Academic Press, London, pp 35–54

Mezger EM, De Nooijer LJ, Boer W, Brummer GJA, Reichart GJ (2016) Salinity controls on Na incorporation in Red Sea planktonic foraminifera. Paleoceanography 31(12):1562–1582

Muñoz-Marín MC, López-Lozano A, Moreno-Cabezuelo JÁ, Díez J, García-Fernández JM (2024) Mixotrophy in cyanobacteria. Curr Opin Microbiol 78:102432. https://doi.org/10.1016/j.mib.2024.102432

Murray JW (2006) Ecology and applications of benthic foraminifera. Cambridge University Press, Cambridge

Noffke N, Awramik SM (2026) A tale of two microbialites: stromatolites and microbially induced sedimentary structures. Sedimentology. https://doi.org/10.1111/sed.70109

Orszag-Sperber F, Harwood G, Kendall A, Purser BH (1998) A review of the evaporites of the Red Sea–Gulf of Suez rift. In: Purser BH, Bosence DWJ (eds) Sedimentation and tectonics in rift basins: Red Sea–Gulf of Aden. Chapman & Hall, London, pp 409–426. https://doi.org/10.1007/978-94-011-4930-3_22

Pei Y, Suarez-Gonzalez P, Duda J-P, Reitner J (2024) Organic matter influence on ooid formation: new insights into classic examples (Great Salt Lake, USA; Triassic Germanic Basin, Germany). Sedimentology 71:1419–1435. https://doi.org/10.1111/sed.13179

Pellaton C (1982) Geologic map of the Umm Lajj Quadrangle, sheet 25B, Kingdom of Saudi Arabia, GM-61A. Ministry of Petroleum and Mineral Resources, Deputy Ministry for Mineral Resources.

Pensa T, Baby G, Teillet T, Delaunay A, Delgado-Huertas A, Afifi AM (2025) Evolution of carbonate platforms in the northeast Red Sea during the last 23 million years. Sci Rep 15:10332. https://doi.org/10.1038/s41598-025-92219-x

Perrin C, Plaziat J-C, Rosen BR (1998) Miocene coral reefs and reef corals of the south-western Gulf of Suez and north-western Red Sea: distribution, diversity and regional environmental controls. In: Purser BH, Bosence DWJ (eds) Sedimentation and tectonics in rift basins: Red Sea–Gulf of Aden. Chapman & Hall, London, pp 296–319. https://doi.org/10.1007/978-94-011-4930-3_17

Peters SE, Husson J, Wilcots J (2017) Rise and fall of stromatolites in shallow marine environments. Geology. https://doi.org/10.1130/G38931.1

Petrovic A, Panara Y, Vahrenkamp V (2023) Morphological evidence for the extension of the Zabargad transform Fault Zone to the Saudi Arabian Red Sea margin. J Geol Soc. https://doi.org/10.1144/jgs2023-009

Pisapia C, Mateu-Vicens G, Benzoni F, Westphal H (2024) Mediterranean imprint on coral diversity in the incipient Red Sea (Burdigalian, Saudi Arabia). Palaios 39:233–242. https://doi.org/10.2110/palo.2023.025

Polgári M, Gyollai I (2021) Geochemical constraints on the element enrichments of microbially mediated manganese and iron ores – an overview. Ore Geol Rev 136:104203. https://doi.org/10.1016/j.oregeorev.2021.104203

Purser BH, Plaziat JC, Rosen BR (1996) Miocene reefs of the northwest Red Sea. In: Franseen EK, Esteban M, Ward WC, Rouchy JM (eds) Models for Carbonate Stratigraphy from Miocene Reef Complexes of Mediterranean Regions, Soc. Econ. Paleont. Miner. Concepts Sedimentology Paleontology, pp 347–366, Tulsa

Purser BH, Plaziat J-C (1998) Miocene periplatform slope sedimentation in the north-western Red Sea rift, Egypt. In: Purser BH, Bosence DWJ (eds) Sedimentation and tectonics in rift basins: Red Sea–Gulf of Aden. Chapman & Hall, London, pp 320–346. https://doi.org/10.1007/978-94-011-4930-3_18

Rasul NMA, Stewart ICF, Nawab ZA (2015) Introduction to the Red Sea: its origin, structure, and environment. In: Rasul NMA, Stewart ICF, Nawab ZA (eds) *The Red Sea* – the formation, morphology, oceanography and environment of a young ocean basin. Springer, pp 1–28

Reid RP, Macintyre IG, Browne KM, Steneck RS, Miller T (1995) Modern marine stromatolites in the Exuma Cays, Bahamas: uncommonly common. Facies 33:1–17. https://doi.org/10.1007/BF02537442

Reid RP, MacIntyre IG, Steneck RS (1999) A microbialite/algal ridge fringing reef complex, Highborne Cay, Bahamas. Atoll Res Bull 466:1–18

Reid RP, Suosaari EP, Oehlert AM, Pollier CGL, Dupraz C (2024) Microbialite accretion and growth: lessons from Shark Bay and the Bahamas. Annu Rev Mar Sci 16:487–511. https://doi.org/10.1146/annurev-marine-021423-124637

Reitner J (2004) Organomineralization. In: Seckbach J (ed.) Origins. Cellular Origin, Life in Extreme Habitats and Astrobiology, vol 6, Springer, Dordrecht. https://doi.org/10.1007/1-4020-2522-X_13

Reitner J, Neuweiler F, Gautret P (1995) Part II modern and fossil automicrites: implications for mud mounds genesis. Facies 32:4–17

Riding R (2000) Microbial carbonates: the geological record of calcified bacterial-algal mats and biofilms. Sedimentology 47:179–214

Riding R (2002) Microbial carbonates: the geological record of calcified bacterial–algal mats and biofilms. Sedimentology 47(1):179–214

Schiebel R, Hemleben C (2017) Planktonic foraminifers in the modern ocean. Springer, Berlin. https://doi.org/10.1007/978-3-662-50297-6

Schultze-Lam S, Fortin D, Davis BS, Beveridge TJ (1996) Mineralization of bacterial surfaces. Chem Geol 132(1–4):171–181

Segev A, Avni Y, Shahar J, Wald R (2017) Late Oligocene and Miocene different seaways to the Red Sea-Gulf of Suez rift and the Gulf of Aqaba-Dead Sea basins. Earth Sci Rev 171:196–219. https://doi.org/10.1016/j.earscirev.2017.05.004

Sellanes J, Gorny M, Zapata-Hernández G, Alvarez G, Muñoz P, Tala F (2021) A new threat to local marine biodiversity: filamentous mats proliferating at mesophotic depths off Rapa Nui. PeerJ 9:e12052. https://doi.org/10.7717/peerj.12052

Shen Y, Thiel V, Duda J-P, Reitner J (2018) Tracing the fate of steroids through a hypersaline microbial mat (Kiritimati, Kiribati/Central Pacific). Geobiology 16(3):307–318. https://doi.org/10.1111/gbi.12279

Stephen RP, Michael TA, Charles RB, William BM, David JR, David MS, Andrei T, Mark VW (2005), Preferential deposition and preservation of structurally-controlled synrift reservoirs: Northeast Red Sea and Gulf of Suez: GeoArabia, v. 10, p. 97–124. https://doi.org/10.2113/geoarabia100197

Stern RJ, Johnson PR (2019) Constraining the opening of the Red Sea: evidence from the Neoproterozoic margins and Cenozoic magmatism for a volcanic rifted margin. In: Rasul NMA, Stewart ICF (eds) Geological setting, palaeo-environment and archaeology of the Red Sea. Springer, pp 53–81

Suarez-Gonzalez P, Benito MI, Quijada IE, Mas R, Campos-Soto S (2019) Trapping and binding': a review of the factors controlling the development of fossil agglutinated microbialites and their distribution in space and time. Earth Sci Rev 194:182–215. https://doi.org/10.1016/j.earscirev.2019.05.007

Suarez-Gonzalez P, Benito MI, Arenas C, Pomar L (2022) Columnar microbialites of the upper Miocene of Mallorca (Spain): a new morphogenetic model based on concurrent accretion and bioturbation – uncommon or overlooked? Sedimentology 69:88–120

Suosaari EP, Reid RP, Playford PE, Foster JS, Stolz JF, Casaburi G, Hagan PD, Chirayath V, Macintyre IG, Planavsky NJ, Eberli GP (2016) New multi-scale perspectives on the stromatolites of Shark Bay, Western Australia. Sci Rep 6:20557. https://doi.org/10.1038/srep20557

Torfstein A, Steinberg J (2020) The Oligo-Miocene closure of the Tethys Ocean and evolution of the proto-Mediterranean Sea. Sci Rep 10:1–10. https://doi.org/10.1038/s41598-020-73009-7

Trichet J, Défarge C (1995) Non-biologically supported organomineralization. Bulletin de l'Institut Océanographique (Monaco) Numéro Spécial 14:203–236

Tubbs RE, Fouda HGA, Afifi AN, Raterman NS, Hughes GW, Fadolalkarem YK (2014) Midyan Peninsula, northern Red Sea, Saudi Arabia: Seismic imaging and regional interpretation. GeoArabia, 19 (3), 165-184. https://doi.org/10.2113/geoarabia1903165

Vahrenkamp V, Chandra V, Garuglieri E, Marasco R, Hachmann K, Khanna P, Daffonchio D, Petrovic A (2024) Discovery of modern living intertidal stromatolites on Sheybarah Island, Red Sea, Saudi Arabia. Geology 52:347–351. https://doi.org/10.1130/G51793.1

Vasconcelos C, McKenzie JA (1997) Microbial mediation of modern dolomite precipitation and diagenesis under anoxic conditions (Lagoa Vermelha, Rio de Janeiro, Brazil). J Sediment Res 67:378–390

Villafañe PG, Corbí H, Cónsole-Gonella C, Ruiz-Sánchez FJ, Soria JM (2018) The Messinian stromatolites of the Sierra del Colmenar

(Western Mediterranean): facies characterization and sedimentological interpretation. PeerJ 6:e5766. https://doi.org/10.7717/peerj.5766

Vogt C, Lauterjung J, Fischer RX (2002) Investigation of the clay fraction (<2 µm) of the Clay Mineral Society reference clays. Clays Clay Miner 50(3):388–400

Warthmann R, Vasconcelos C, Bittermann AG, McKenzie JA (2011) The role of purple sulphur bacteria in carbonate precipitation of modern and possibly early Precambrian stromatolites. In: Reitner J (ed) Advances in Stromatolite Geobiology. Lecture Notes in Earth Sciences, vol 131. Berlin, Heidelberg: Springer, pp 379–394 https://doi.org/10.1007/978-3-642-10415-2_9.

Westall F, Steele A, Toporski J, Walsh M, Allen C, Guidry S, Chafetz H (2000) Polymeric substances and biofilms as biomarkers in terrestrial materials: implications for extraterrestrial samples. J Geophys Res Planets 105(E10):24511–24527

Zankl H (1993) The origin of high-Mg-calcite microbialites in cryptic habitats of Caribbean coral reefs - their dependence on light and turbulence. Facies 29:55–60